AIAA Propulsion and Energy Forum
10-12 July 2017, Atlanta, GA
53rd AIAA/SAE/ASEE Joint Propulsion Conference

10.2514/6.2017-4629

Experimental Studies of the Helicon Injected Inertial Plasma Electrostatic Rocket (HIIPER)

Drew Ahern[1], Hussein Al-Rashdan[2], Oguzhan Altun[2], Grant Berland[2], Emil Broemmelsiek[2], Zhengyu Chen[2], Patchara Choakpichitchai[2], Zongxu Dong[2], Patrick Drew[2], Nicklaus Richardson[2], Nicholas St.Lawrence[2], Kyle Stanevich[2], Albert Valiaveedu[3], and George Miley[4]
University of Illinois at Urbana-Champaign, Urbana, IL, 61801

The Helicon Injected Inertial Plasma Electrostatic Rocket (HIIPER) is a space propulsion concept using a helicon plasma source and grids from inertial electrostatic confinement (IEC) fusion theory. The helicon source generates a dense plasma, and the IEC grids extract the ions, producing a thrust. A unique feature of this setup is that the IEC grids are designed to also produce a jet of electrons, resulting in a neutralized plasma exhaust. In this study, a Langmuir probe and a Mach probe have been placed at the interface between the helicon and grid system, and a retarding potential analyzer (RPA) has been placed downstream. Langmuir probe results show electron temperatures ranging from 15 to 30 eV, depending on the bias potential of the helicon plasma. Mach probe results provide some preliminary data on the Mach number. RPA results indicate that ions are exiting with energies approximately equal to the bias potential of the helicon plasma. RPA results also show that high energy electrons are present when a potential of a few negative kV is applied to the IEC grid system. These results are encouraging, suggesting that the basic concept behind HIIPER is sound.

Nomenclature

HIIPER	=	Helicon Injected Inertial Plasma Electrostatic Rocket
IEC	=	inertial electrostatic confinement
RF	=	radio frequency
RPA	=	retarding potential analyzer

I. Introduction

A novel electric propulsion design is being studied which combines two separate plasma concepts: the helicon plasma source, which is a well-known method to efficiently generate a plasma,[1] and inertial electrostatic confinement (IEC). IEC is a fusion concept that has received considerable study as a fusion neutron source for application in neutron activation analysis.[2] The basic IEC configuration consists of a spherical metal grid located inside a spherical metal vacuum chamber. The metal grid configuration can vary, but generally it can be thought of as metal wires spot welded into the form of a sphere, in a pattern similar to the lines on a basketball or soccer ball. Gas at a pressure of a few mTorr is input into the chamber, and the grid is biased to a negative potential on the order of tens of kV. Plasma forms between the grid and the chamber via Paschen's law, and the resulting positive ions accelerate inward toward the negative grid. These ions either recirculate through the grid, or they collide with the grid or other ions/neutrals, resulting in fusion reactions if a fissionable gas such as deuterium is used. It has been observed that making one of the IEC grid openings larger than the rest results in the formation of a beam (termed a "plasma jet") that flows out of this asymmetry. Experiments indicate this beam is electron dominated,[3] with the source of the electrons being thermal emission or secondary electron emission from grid impacts or ionization events in the grids. In a space thruster, this electron emission is theorized to function in neutralizing an ion exhaust.

---

[1] PhD candidate, Department of Aerospace Engineering. Student member, AIAA.
[2] Undergraduate research assistant, Department of Aerospace Engineering.
[3] Undergraduate research assistant, Department of Mechanical Science and Engineering.
[4] Professor emeritus, Department of Nuclear, Plasma, and Radiological Engineering. Associate fellow, AIAA.

According to Paschen's law, plasma generation via an IEC system requires a certain gas pressure in the chamber, so generating a plasma by an IEC setup alone in space is extremely difficult. However, plasma can also be injected externally from a separate plasma source, removing pressure dependence. This leads to the Helicon Injected Inertial Plasma Electrostatic Rocket (HIIPER), which consists of a helicon plasma source for plasma generation and two concentric asymmetric IEC grids for ion extraction and acceleration. In this configuration, the inner grid is biased negatively while the outer grid is floating. The IEC grids are being studied in extracting ions from the helicon source while also providing a neutralizing electron beam for the extracted ions. Additionally, the IEC grid configuration is being studied for producing minimal ion divergence, with the idea being that any ions extracted off-axis of the thrust vector will recirculate through the grids until either hitting a grid wire or leaving through the asymmetry.

Helicon plasma sources can achieve relatively high plasma densities of up to 10^{14} cm^{-3},[1] and therefore they are attractive for space propulsion purposes if an efficient method to extract the plasma is developed. Numerous thruster designs consisting of helicon sources by themselves have been tested (relying on double layer physics, e.g., as done by West et al[4]), though results have mostly shown low efficiencies. One method attempted by Williams and Walker used ion thruster grids with a helicon plasma generation stage.[5] Results indicated low performance but had the possibility of improvement through further optimization of the grid system. HIIPER is another prospective extraction method, with the ion thruster grids replaced by IEC grids, potentially offering ion exhaust neutralization and low divergence. Studies of the HIIPER method are presented here.

II. Study description

A. Experimental facilities and setup

Experiments are being conducted in a 61 cm diameter stainless steel vacuum chamber that is connected to a 1.5" outer diameter quartz tube where argon is injected. The vacuum chamber has a base pressure of 10^{-5} Torr. During testing, the argon mass flow rate is typically kept to 3 sccm (approx. 0.1 mg/s), which results in a chamber pressure of approximately 7 x 10^{-5} Torr. Argon gas pressure is also read upstream of the helicon section, and it is typically ~6 mTorr.

The argon is ionized by a helicon antenna that is wrapped around the outside of the quartz tube. This helicon antenna is in an m = +1 configuration, and it is connected to an automatic L-type matching network fed by an RF power supply. RF power is typically kept to 300 W and at maximum is limited to 500 W due to heating issues. The operating frequency of the helicon is 13.56 MHz. Water-cooled electromagnets surround the helicon section, and they can reach a maximum axial magnetic field of 1,200 G. A diagram of the experiment is shown in Figure 1. It should also be noted that helicon mode was not experimentally verified in these tests, so in actuality the helicon source may have been run at inductively coupled mode.

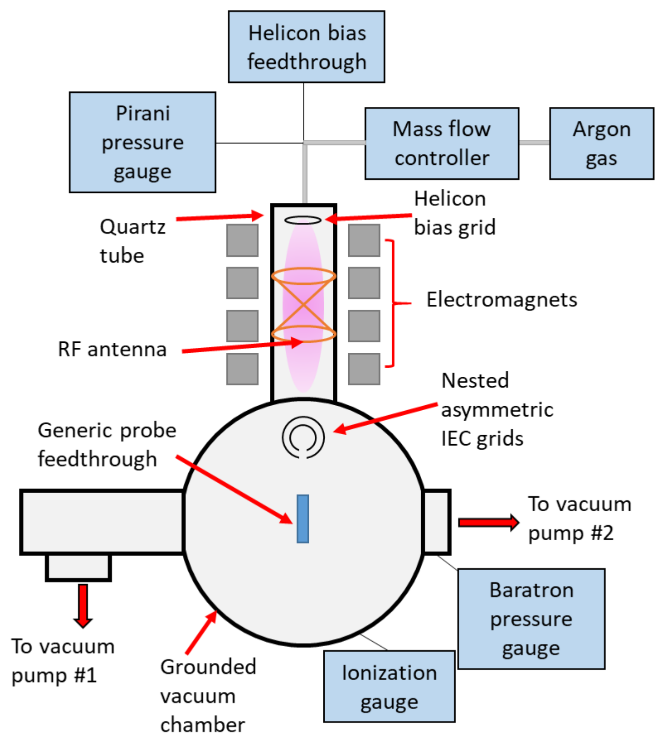

Figure 1. Experiment diagram. Components are in blue boxes.

On the upstream end of the helicon section immediately before the electromagnets, a circular metal meshed grid of approximately 1" ⌀ has been placed. This grid is shown in Figure 2a. Prompted by earlier studies,[5] this grid on the upstream end of the helicon section is biased to positive voltages to increase the downstream flow velocity. This approach is also consistent with ion sources being used for plasma processing purposes, where biasing the plasma source to a positive potential is necessary to increase the exhaust energy.[6] In these HIIPER experiments, this grid is biased up to 180 V, which is a limit set by the power source (two DC power supplies in series). Additionally, it should be noted that a meshed grid was chosen as the bias device (as opposed to a circular metal plate) due to the setup of the experiment, i.e., the helicon source is uniquely connected to the argon gas input, and having a metal plate instead of a mesh could possibly impede the gas flow into the helicon tube.

At the exit of the helicon section is the IEC grid setup. In this study, two separate configurations of nested concentric grids were tested. The first setup utilized two spherical grids similar to IEC grids but with less wires, shown in Figure 2b. These grids were termed "gridlets" to differentiate them between the IEC grids. The purpose of using these gridlets instead of IEC grids was that these gridlets were hollow enough to let probes pass through them to the upstream side at the helicon-grid interface. This allowed for measuring upstream parameters of the plasma while varying gridlet potential, i.e., the gridlets mimicked to some degree the effects of IEC grids. The second setup consisted of two IEC grids with diameters of 14 cm and 7 cm, shown in Figure 2c. The larger size was chosen to match previous experiments, and the smaller size was chosen to fit inside the larger grid. Plasma parameters downstream of the helicon-IEC grid setup were then measured.

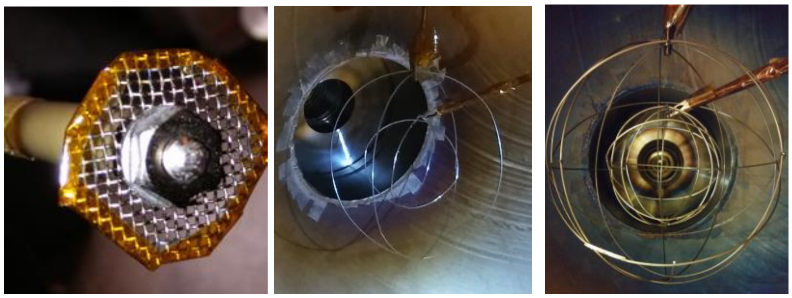

a) b) c)

Figure 2. a) Upstream helicon bias grid. Kapton tape on edges is to prevent grid from accidentally scratching helicon quartz tube during installation. b) "Gridlets" used for measurement of upstream plasma parameters at helicon-grid interface. c) Concentric asymmetric IEC grids, with asymmetries facing the viewer.

B. Diagnostics

Three diagnostics have been employed in this study. A Langmuir probe and a Mach probe were used with the gridlet setup to measure upstream properties of the plasma at the helicon-grid interface. The Langmuir probe measured electron temperature and plasma potential, and the Mach probe measured Mach number. A retarding potential analyzer (RPA) was used with the IEC grid setup to measure downstream properties of the helicon-grid system. Most importantly, the RPA has allowed for understanding the composition of the exhaust, specifically the ion and electron energy contributions. Additionally, the most probable ion potential was analyzed with the RPA. Details of these diagnostics are described below.

1. *Langmuir probe*

The Langmuir probe is an RF compensated design based off of Sudit,[7] and the design has previously been used in similar helicon characterization studies of this type of helicon setup.[8] The probe consists of four notch filters in alternating order: two to block the fundamental frequency of 13.56 MHz and two to block the harmonic frequency of 27.12 MHz. Each filter was constructed with an inductor and capacitor in parallel, with inductance and capacitance values chosen to block the respective frequency. It should be noted that due to component tolerances, many pairs were tested to get as close to the desired frequency values as possible. A diagram of the circuit is shown in Figure 3a. The probe tip was made of tungsten of 0.254 mm diameter with a tip length of 7 mm (fairly long to reduce probe shadowing effects). A compensation electrode was also included, consisting of tungsten wire wrapped

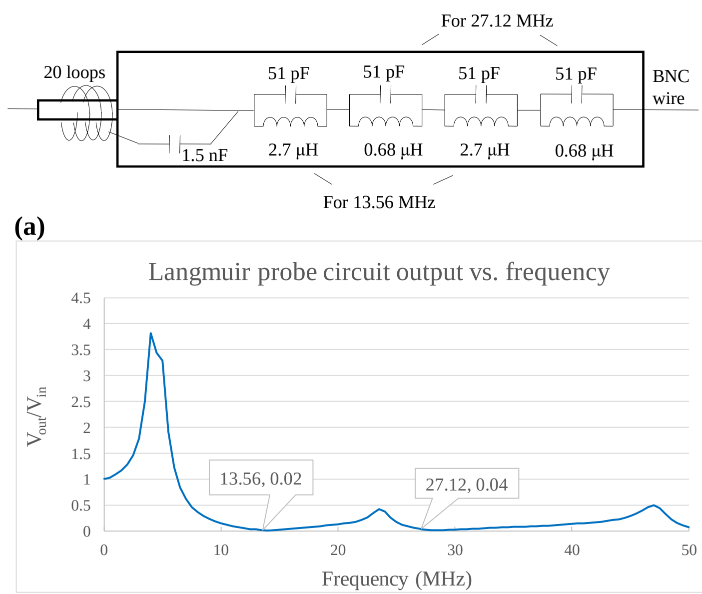

Figure 3. a) Langmuir probe design. b) Filter response at different frequencies.

approximately 20 times near the probe tip and attached to a capacitor in parallel with the probe tip. A plot of the Langmuir probe circuit output at different input frequencies is shown in Figure 3b.

During testing, the probe was biased with a function generator and bipolar operational amplifier, and the resulting current and voltage were read across a resistor using an oscilloscope. Current and voltage data were then smoothed and analyzed using a MATLAB code.

2. Mach probe

A Mach probe was included to measure the Mach number at the helicon-grid interface. In general, a Mach probe consists of two probe tips similar to a Langmuir probe, where the tips are partially separated by an insulator. These probe tips are biased to ion saturation potential. When immersed in a plasma, the ratio of the currents of the two probe tips provides an estimate for the Mach number of the flow, according to the equation

$$\frac{J_{up}}{J_{down}} = \exp(KM) \quad (1)$$

where J_{up} and J_{down} are the respective upstream and downstream currents, M is the Mach number, and K is a calibration factor that depends on the experiment. Using various computational models, values of K have been tabulated for different conditions, such as unmagnetized vs. magnetized and collisions vs. collisionless conditions.[9] For this experiment, a K value of 1.34 was used. When comparing upstream Mach probe data with downstream data measured by the retarding potential analyzer (RPA), an estimate of an ion's acceleration can be determined.

Two different probes were tested in this setup: a perpendicular Mach probe consisting of two orthogonal probe tips, and a parallel Mach probe consisting of two parallel probe tips. In the perpendicular Mach probe, two insulated probe tips are positioned perpendicularly to each other, with one tip facing the plasma flow direction. Insulation surrounds each probe tip so that only the probe tip's face is visible. The perpendicular Mach probe used in this study is shown in Figure 4a. Note that the wires used were copper wires of 1.3 mm ⌀. With a perpendicular Mach probe, Ando derived and experimentally validated equations to calculate the Mach number and hence the ion speed.[10] Perpendicular Mach probes have been used previously in other helicon thruster experiments;[11] however, in HIIPER tests, problems were encountered where the perpendicular probe tip measured higher currents than the parallel probe tip. That is, the tip facing the plasma flow direction had a smaller current than the tip perpendicular to it. This was thought to be due to ion motion along the magnetic field lines, resulting in a higher current on the perpendicular probe face. Additionally, the non-zero distance between the two tips was thought to have resulted in poor correlation between the two currents. Therefore, a parallel Mach probe was subsequently implemented, resulting in better 1-D measurements of the ion flow. The parallel Mach probe is shown Figure 4b, where the probe tips extend approximately 1 mm from the ceramic holder.

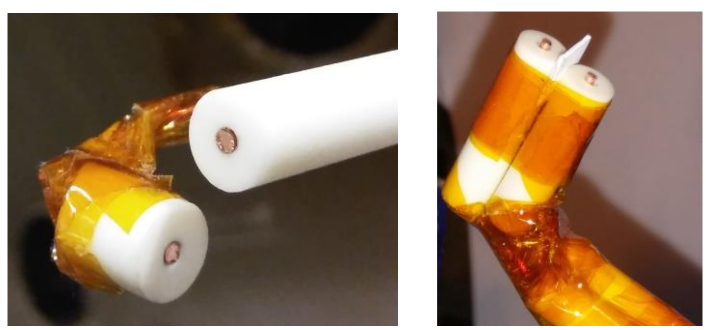

a) b)

Figure 4. a) Perpendicular Mach probe. b) Parallel Mach probe.

3. Retarding potential analyzer (RPA)

While the Langmuir and Mach probes were used to measure plasma properties upstream, an RPA was used to measure the downstream properties of the IEC grid system. By selectively filtering particles through a series of meshed grids at various electrical potentials, the RPA can determine whether ions are being accelerated through the IEC grids and whether high energy electrons accompany these ions. The RPA used in this study is based off of two designs: a design used by Shabshelowitz for a helicon Hall thruster[12] and an earlier design used for HIIPER.[13] In particular, the spacing of the various grids and the grid mesh size were used from the design by Shabshelowitz, and the overall form was built from the previous HIIPER RPA.

The RPA consists of 3" by 3" Macor square sheets, and the overall design of the RPA is shown in Figure 5. The 316 stainless steel meshed grids have openings of 0.28 mm wide with a wire diameter of 0.10 mm. Machined

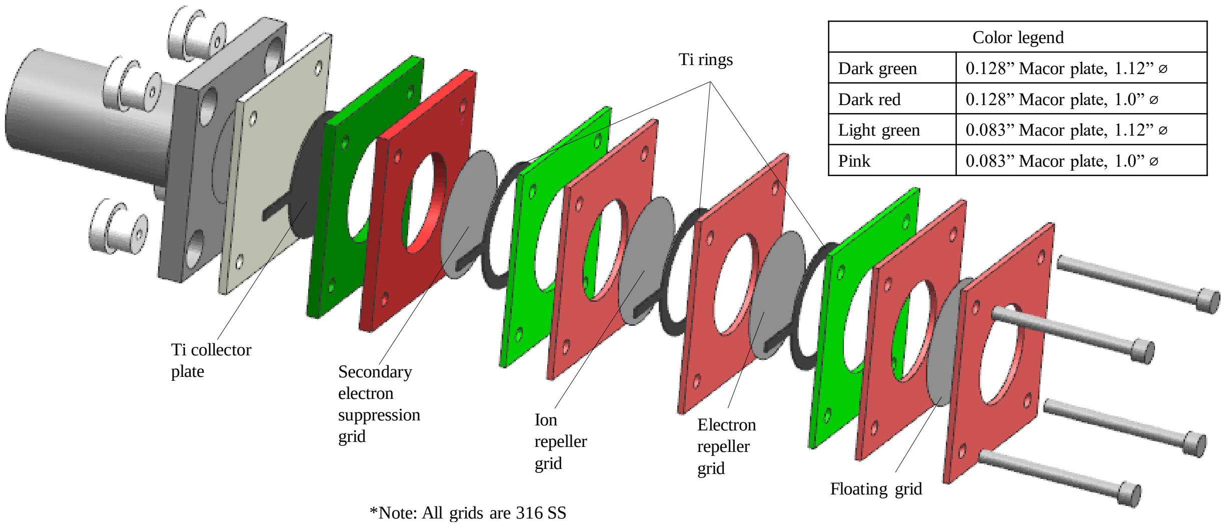

Figure 5. RPA exploded view.

titanium rings hold the grids and allow for electrical connections to bias the grids. A titanium collector plate at the rear of the RPA measures the resulting current. In contrast to the design by Shabshelowitz which did not include a secondary electron suppression grid, one was included in these tests. Also, the previous HIIPER RPA had issues involving sputtered metal coating the inside channel of the RPA, resulting in arcing between the grids. To prevent this from happening, the central hole diameters of adjacent Macor spacers were slightly different to prevent a conducting path from forming between the grids.

During the testing of the RPA, the outer IEC grid was left floating, and the inner IEC grid was varied from -0.3 kV to up to -4 kV. In prior tests of an IEC grid operating at glow discharge mode, an electron beam with a potential similar to the IEC grid potential was observed. Therefore, the electron repeller grid on the RPA was set to several different negative voltages for each inner IEC grid potential tested. For each test, the ion repeller grid was swept from 0 to 975 V (limit of power supply’s sweep voltage) over approximately 100 s. The secondary electron suppression grid was set to -9 V with a battery. The collector plate was connected to ground, and the plate current was measured across a resistor using a data acquisition device. The resulting currents from each test were compared, and particular attention was paid to whether these currents changed when the IEC grid potential was kept constant but the RPA electron repeller grid voltage was changed.

III. Results and discussion

Results from these experiments are described below. Note: the inner grid (either the gridlet or the IEC grid) is always biased negative, the RPA electron repeller grid is always biased negative, the ion repeller grid is always biased positive, and the helicon bias grid is always biased positive. By convention, these voltages are sometimes referred to without specifying negative or positive signs.

A. Langmuir probe measurements

Several magnetic field values were tested with the Langmuir probe and the gridlet configuration, with the probe placed at the interface between the helicon and the gridlets. For each of the magnetic fields tested, the inner gridlet voltage was varied, and data from the Langmuir probe was collected. The helicon bias grid was set to a voltage of 180 V but was varied occasionally, as described below.

In testing the Langmuir probe at different magnetic fields, results that could be interpreted with standard Langmuir probe analysis were only found when the magnetic field was 90 G. This is possibly due to the positively biased grid placed at the upstream end of the helicon source. The current on this bias grid was recorded, and though it was independent of the voltage on the downstream gridlet, it was observed to be very dependent on the magnetic field and somewhat dependent on the bias voltage. This is shown in Table 1. It is likely that at certain magnetic fields, the field lines pass through the bias grid in a certain way that causes a large amount of electrons to collide with it. To maintain charge neutrality, ions must travel downstream. Another possible reason for the “optimum” 90 G magnetic field is that at other magnetic field values, the plasma may follow magnetic field lines that intersect with a chamber wall, causing the plasma to be lost due to collisions with the walls.

Table 1. Current read by the helicon bias supply at various magnetic fields and bias voltages.

Magnetic field (G)	45	90			135	300	900
Bias voltage (V)	180	90	135	180	180	180	180
Bias current (A)	0.04	0.09	0.12	0.11	0.02	0.00	0.01

The electron temperature at 90 G was calculated at different bias voltages and gridlet voltages. These results are shown in Figure 6. The electron temperature values were observed to be very dependent on the bias grid voltage, with higher electron temperatures associated with more positive biases. Having a more positive bias is also associated with higher energy ions; these higher energy ions likely collide with the gridlets, producing secondary electrons that have energies corresponding with incident ion energies. Additionally, higher electron temperatures were also somewhat associated with more negative gridlet voltages. This is also possibly due to the ions having an increased speed when hitting the gridlets, resulting in secondary electrons with greater energy. Current on the gridlet power supply was also observed to increase with gridlet voltage, indicating that more ions were colliding with the gridlets. Regarding error for the electron temperatures, a standard 20% error was assumed.[14]

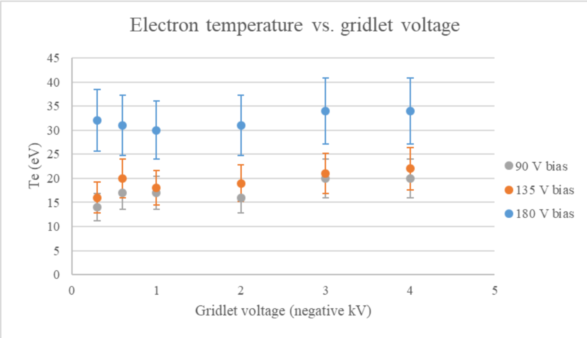

Figure 6. Electron temperature vs. gridlet voltage.

Finally, plasma potentials were calculated, and they were shown to be approximately constant while varying gridlet voltage, however they increased with increasing bias voltage. On average, the plasma potentials were 37 V, 56 V, and 71 V for bias voltages of 90 V, 135 V, and 180 V, respectively. Further analysis using an emissive probe is needed to verify these values.

B. Mach probe measurements

The Mach probe was run for several magnetic field values, and for each magnetic field, the gridlet voltage and the bias voltage were varied. (Note: the bias voltages used were slightly different than those used in other tests, but overall trends in results are the same.) Data on the currents of the two probe tips were then collected. From these experiments, it was found that for larger magnetic fields (180 and 300 G), the Mach probe tip on the downstream side of the Mach probe measured a current higher than that of the tip on the upstream side. This has been observed in other works,[15] and for our purposes, this prohibited computation of a Mach number using Eq. (1). Therefore, with the knowledge from the Langmuir probe tests that 90 G is the optimal magnetic field, calculating velocity information at these magnetic fields was skipped.

At 90 G, probe tip currents were measured, and Mach numbers were estimated. The resulting Mach numbers for various gridlet and bias voltages are shown in Figure 7. This data indicates that higher Mach numbers are achieved with higher bias voltages and higher gridlet voltages. It was also noted that the absolute values of the probe tip currents decreased while increasing the bias voltage. This might be due to the ions having a higher energy, preventing some of them from being drawn to the negatively biased Mach probe tips, which were kept constant at approximately -64 V. Magnetic fields of 45 and 135 G (closer in value to 90 G than the 180 and 300 G tests) were also tried. Overall, the Mach numbers for these magnetic fields were sometimes comparable to the 90 G results, however their corresponding probe currents were smaller, indicating that less ions were exiting the source at these conditions.

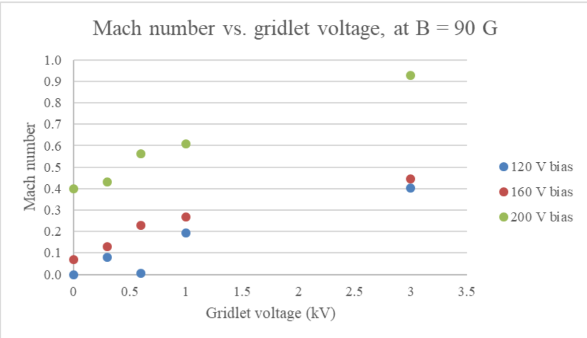

Figure 7. Mach numbers for 90 G magnetic field.

More tests are being conducted with the Mach probe, and a larger data set, as well as error estimates, are in progress.

C. RPA measurements

There were several types of tests run with the RPA and the experiment in the IEC grid configuration. These different tests are described below in their respective sections.

1. Using the RPA to determine most probable ion potential

By sweeping the ion repeller voltage and measuring the resulting current on the collector plate of the RPA, a current-voltage trace is generated. By calculating the slope of the I-V trace, the most probable ion potential can be determined.[16] The RPA was used in this study to verify that different helicon bias voltages result in different downstream potentials. Three biases were tested at a magnetic field of 90 G, and an inner IEC grid voltage of 2 kV was chosen. The resulting smoothed I-V traces for these experiments are shown in Figure 8.

Using a MATLAB code to smooth and analyze the data, most probable ion potentials of 94 V, 151 V, and 204 V were calculated for the biases 90 V, 135 V, and 180 V, respectively. The error of Shabshelowitz's RPA (which HIIPER'S RPA was based off of) in calculating the most probable potential was estimated at ±10 V.[17] Error was also stated to be quantified as the half width at half maximum amount, which is approximately ±40 V for the potentials reported here.

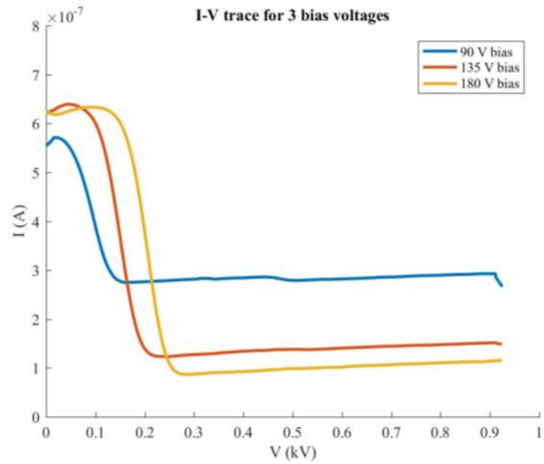

Figure 8. RPA results with different helicon biases.

From these results, the measured most probable ion voltage follows the bias voltage very well. Because a bias of 180 V results in the highest ion voltage, a bias of 180 V was used in most of the subsequent tests.

2. RPA tests with 90 G magnetic field

Tests using the RPA were conducted at a magnetic field of 90 G, where voltages of the inner IEC grid and the electron repeller grid were varied. The goal was to determine the effect of these voltages on the I-V curves. Figure 9 shows the resulting graphs, where each graph represents a separate inner IEC grid voltage, where multiple electron repeller grid voltages were tested. Note that for all analyses of RPA, raw data was smoothed using a Savitzky-Golay filter in MATLAB.

At 0.3, 0.6, and 1 kV of the inner IEC grid, relatively small currents were measured compared to currents at 2, 3, and 4 kV. This might indicate that the IEC grid is a better extractor at higher voltages, and it seems to be optimized around 2 or 3 kV. Also at these higher voltages, it is shown that by increasing the electron repeller grid voltage, the resulting plate current increases. This seems to indicate that high energy electrons are present in the exhaust, similar to what was measured previously with IEC grid glow discharge tests. The source of these electrons could be secondary electrons from ion impacts with the grids, as the power supply for the inner IEC grid shows a slightly increased current for higher IEC voltage values.

3. RPA tests with other magnetic fields

Results for the other magnetic fields are shown in Figure 10. Note that just the 2kV inner IEC grid tests are being compared here, though other voltages were tested with similar trends. Overall, current is much lower than the currents measured from the 90 G tests. Also in each of these cases, very little change in current is observed by changing the electron repeller voltages. Regarding the power supply current for the inner IEC grid (i.e., not the RPA measured current), for the 45, 135, and 300 G cases, less current was read than what was read during the 90 G tests. This seems to indicate that there were less ions hitting the grid for these non-90 G tests, and therefore less secondary electrons being produced. This agrees with the data in the graphs: not as many high energy electrons are being detected with the RPA. For the 900 G case, a similar inner IEC grid power supply current was read as the 90 G case, but at this high magnetic field, it is likely that the particles are being affected by the magnetic field and not traveling downstream past the grid.

4. Verifying RPA behavior with regard to electrons

The next step was to verify for the 90 G case that the electron repeller grid was not artificially increasing the collector plate current by drawing in more ions as the grid was made more negative. Previously run tests were repeated for 90 G at an inner IEC grid at 2 kV, and the RPA electron repeller grid was varied up to 2.5 kV. By having the electron repeller grid potential equal to the IEC grid potential, the electron repeller grid would theoretically stop all electrons from entering the RPA. Therefore by exceeding the IEC grid potential, no further change would be expected to occur.

Results are shown in Figure 12. Tests at electron repeller grid voltages of 1 and 2 kV were fairly similar to earlier results. As the electron grid was raised to 2.25 and 2.5 kV, the current did not continue increasing. This seems to indicate that high energy electrons are present with energies up to the inner IEC grid voltage, confirming theoretical expectations regarding electrons originating from the IEC grids. It should be noted that for the latter portion of the ion sweeps, the current changes slightly. This is likely due to secondary electrons.[18]

Tests were also attempted for an inner IEC grid at 3 kV, however some arcing occurred that did not occur in earlier tests. It was observed later when opening the chamber and examining the RPA that there was some sputtered material on the RPA meshed grids (likely Kapton tape particles). This was thought to have caused the arcing.

5. RPA tests with IEC grid turned sideways

The next test was to determine whether these high energy electrons were being directed at the RPA from the asymmetry in the IEC grids or elsewhere. To do this, the inner IEC grid was turned 90° to the side, with the asymmetry now pointing perpendicular to the helicon exhaust and RPA inlet. At a magnetic field of 90 G and inner IEC grid at 2 kV, the resulting RPA currents showed no electron components to the currents (see Figure 12), in contrast to when the asymmetry was pointed toward the RPA. This indicates that the electrons formed are exiting the IEC grid's asymmetry.

6. RPA test conclusions

The results from these tests indicate that ions are being extracted from the helicon source that have a most probable potential approximately equal to the helicon bias grid potential. Additionally, high energy electrons are present when the IEC grid is biased to a few negative kV. These electrons appear to originate from the IEC grid's asymmetry, confirming previous experiments in glow discharge mode.

The tests discussed here were conducted with the RPA located in one place. Moving the RPA and repeating the experiments will be necessary to determine how the exhaust varies spatially. Additionally, it should be noted that during testing, the chamber pressure of the experiment was approximately 0.1 mTorr. This will need to be investigated further to determine whether there were any pressure-related effects on the results above.

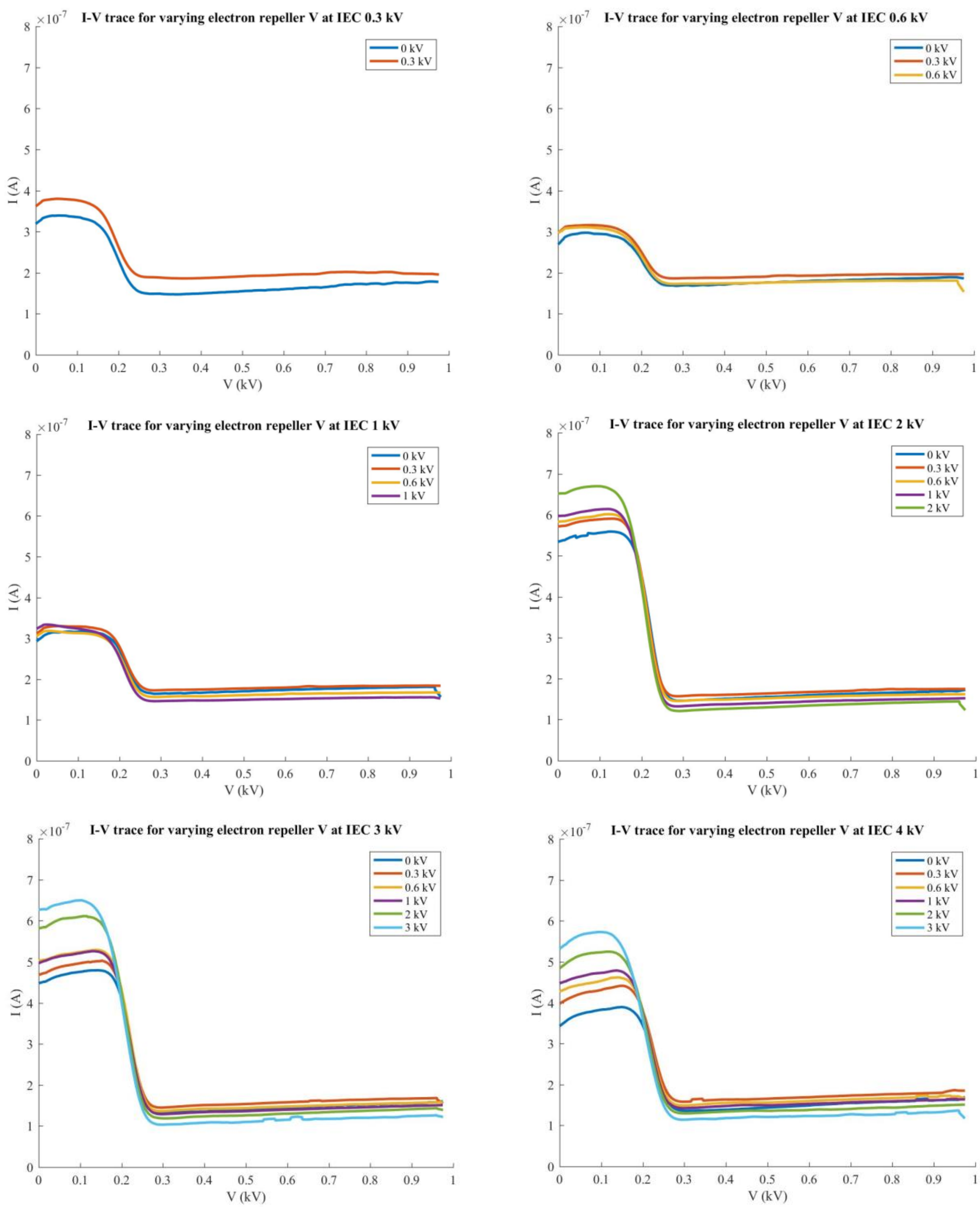

Figure 9. RPA results with helicon electromagnets at 90 G. Collector plate current is on y axis and ion sweep voltage on x axis. For each graph, there are several lines representing different RPA electron repeller grid values.

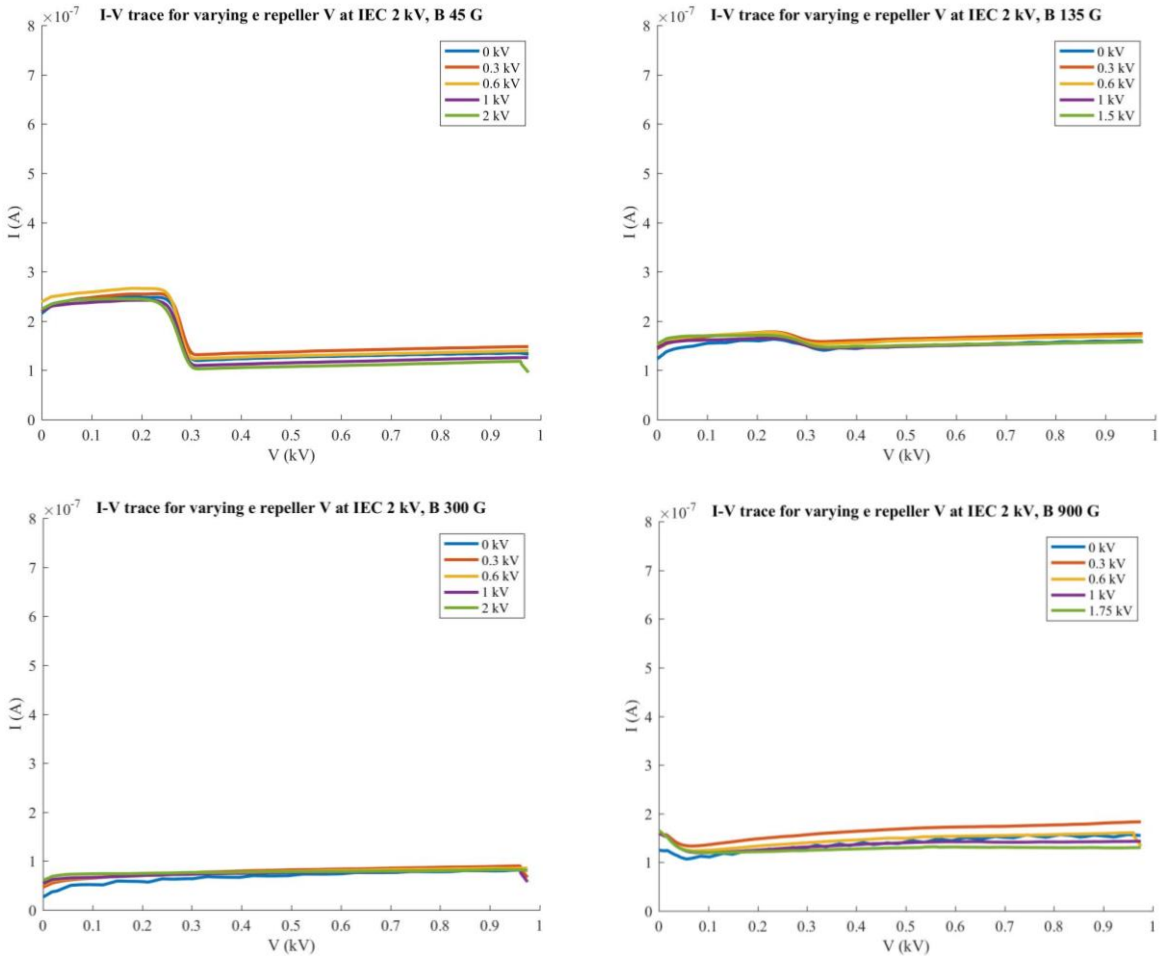

Figure 10. RPA results with inner IEC grid at 2 kV. Each graph corresponds to different helicon electromagnet values.

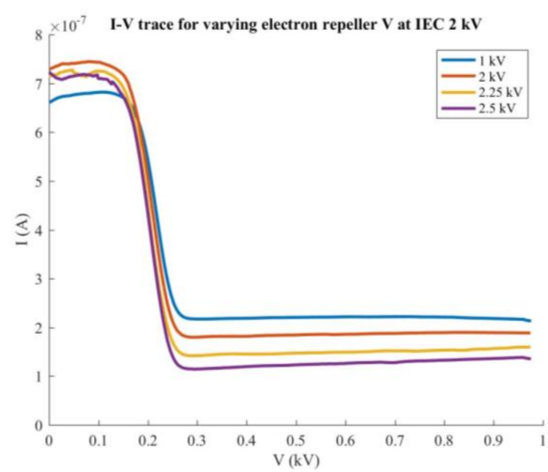

Figure 11. RPA results while running repeller grid at more negative voltages than IEC grid.

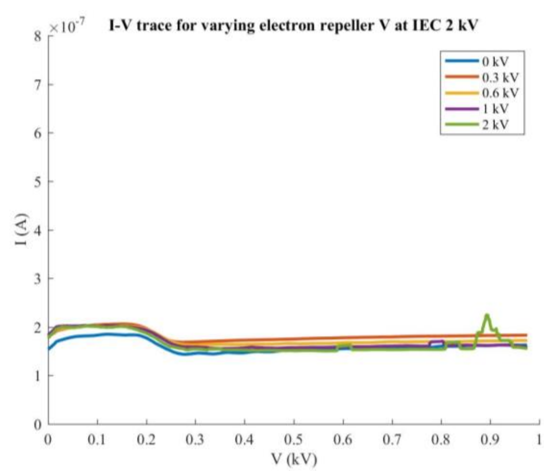

Figure 12. Varying electron repeller grid voltage using IEC grid sideways at 90°.

IV. Ongoing work

A. Experimental

The effect of the placement and shape of the IEC extraction grids are also under study, in addition to the present nested configuration. Theoretically, moving the grids closer to the helicon source exit should extract more ions from the helicon stage. However, interference with the magnetic field configuration should be avoided. Three designs shown in Figure 13 that are attractive conceptually are being tested experimentally. In the first two configurations, extra wires are added to the inner IEC grid to guide more ions out of the asymmetry and draw more ions from the helicon section, respectively. The third configuration consists of a smaller grid system placed further inside the helicon exhaust. Decreasing the distance between the plasma source and the grids may allow more plasma to be extracted, both by the Child-Langmuir law and by reducing ion losses from the magnetic field divergence at the exit of the helicon.

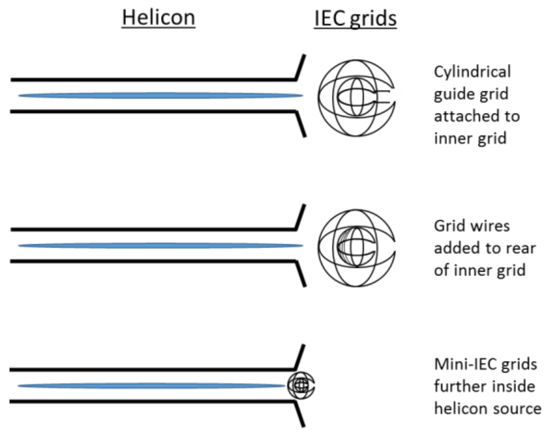

Figure 13. IEC grid configurations to test.

Additionally, diagnostics continue to be implemented with the setup. One of these is an emissive probe to measure the plasma potential along the axis of the exhaust. A second diagnostic being designed is a thrust measurement device which would directly measure the thrust of the exhaust. Current unoptimized thrust estimates of HIIPER are in the sub-millinewton range, and a thrust plate-type design will help confirm this. Taken all together, these results will enable the design of a scaled-up version of HIIPER suitable for space tests.

B. Computational

Concurrently, ion tracking simulations using the computational program COMSOL Multiphysics are being used to assist in the design of the experiment. The IEC grids, the helicon bias grid, the electromagnets, and the geometry of the chamber have been set up in COMSOL. Thus far, simulations have confirmed the most probable ion potential for different grid biases. From experiments with the RPA and the bias grid, the ion most probable potential was calculated to be 94 V and 204 V for bias voltages of 90 V and 180 V, respectively. This corresponds to ion speeds of approximately 31,400 m/s and 21,300 m/s. Figure 14 shows the velocity of ions passing through the simulation's IEC grid setup. In the left picture, a bias of 90 V was used in the helicon section (not shown), and in the right picture, a bias of 180 V was used. Comparing the two results' velocities downstream of the IEC grids, the ion speeds are approximately 10,000 m/s different, matching the experiment.

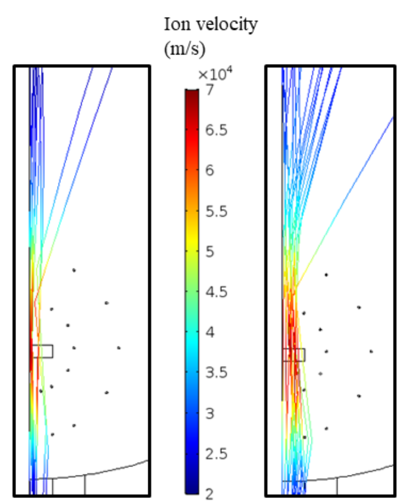

Figure 14. COMSOL particle tracing ion velocity results for 90 V bias (left) and 180 V bias (right).

V. Conclusion

RPA results show that the IEC grid setup has extracted ions with potentials approximately equal to the helicon source's bias potential. Additionally, a population of high energy electrons has been detected exiting the asymmetry of the IEC grid system. Langmuir probe measurements show that electron temperature increases with bias voltage and somewhat with gridlet voltage, indicating that secondary electrons from ion collisions with the grids are the source of the high energy electrons detected with the RPA. Results from the Langmuir probe, Mach probe, and RPA suggest that a magnetic field of 90 G is optimal for HIIPER's current setup. Together, these results validate HIIPER's theorized operation in extracting ions from a helicon source while also generating an electron exhaust. This is very encouraging relative to HIIPER's basic design concept.

Acknowledgments

The authors would like to acknowledge and thank the Air Force Research Lab for generously loaning laboratory equipment for these experiments, and they would also like to thank NASA and National Systems Corp for providing funding for the HIIPER lab. Added support by NPL Associates of Champaign, IL is acknowledged. The authors would also like to thank the machine shops of the Aerospace Engineering Department and Electrical and Computer Engineering Department for their help in making various parts. Additionally, the authors thank Pawel Piotrowicz and Michael Christenson for their assistance with the Langmuir probe and RPA.

References

[1]Chen, F. F., "Plasma ionization by helicon waves," Plasma Physics and Controlled Fusion, Vol. 33, No. 4, 1991, pp. 339-364.

[2]Miley, G. H., and Murali, S. K., *Inertial Electrostatic Confinement (IEC) Fusion Fundamentals and Applications*, Springer, New York, 2014.

[3]Ahern, D., Bercovici, B., Miley G., Chen, G., Ulmen, B., and Keutelian, P., "Advances on the Helicon Injected Inertial Plasma Electrostatic Rocket," AIAA 2014-4172, AIAA SPACE 2014 Conference and Exposition, San Diego, CA, 2014.

[4]West, M. D., Charles, C., and Boswell, R. W., "Testing a Helicon Double Layer Thruster Immersed in a Space-Simulation Chamber," Journal of Propulsion and Power, Vol. 24, No. 1, 2008, pp. 134-141.

[5]Williams, L. T., and Walker, M. L. R., "Initial performance evaluation of a gridded radio frequency ion thruster," Journal of Propulsion and Power, Vol. 30, No. 3, 2014, pp. 645-655.

[6]Brown, I. G. (ed.), *The Physics and Technology of Ion Sources*, 2nd ed., Wiley-VCH Verlag GmbH & Co. KGaA, Weinheim, 2004, p. 32.

[7]Sudit, I. D., and Chen, F. F., "RF compensated probes for high-density discharges," Plasma Sources Sci. Technol., Vol. 3, 1994, pp. 162-168.

[8]Reilly, M. P., "Three Dimensional Imaging of Helicon Wave Fields via Magnetic Induction Probes," Ph.D. Dissertation, Nuclear, Plasma, and Radiological Engineering Dept., University of Illinois at Urbana-Champaign, Champaign, IL, 2009, pp. 76-77.

[9]Chung, K., "Mach probes," Plasma Sources Sci. Technol., Vol. 21, 2012, 063001, pp. 1-47.

[10]Ando, A., Watanabe, T., Watanabe, T., Tobari, H., Hattori, K., and Inutake, M., "Evaluation of Para-Perp Type Mach Probe by Using a Fast Flowing Plasma," J. Plasma Fusion Res., Vol. 81, No. 6, 2005, pp. 451-457

[11]Toki, K., Shinohara, S., Tanikawa, T., Hada, T., Funaki, I., Tanaka, Y., Yamaguchi, A., and Shamrai, K., "On the Electrodeless MPD Thruster Using a Compact Helicon Plasma Source," AIAA 2008-4729, 44th AIAA/ASME/SAE/ASEE Joint Propulsion Conference & Exhibit, Hartford, CT, 2008.

[12]Shabshelowitz, A., Gallimore, A., and Peterson, P., "Performance of a Helicon Hall Thruster Operating with Xenon, Argon, and Nitrogen," Journal of Propulsion and Power, Vol. 30, No. 3, 2014, pp. 664-671.

[13]Ulmen, B., "Formation and Extraction of a Dense Plasma Jet from a Helicon-Plasma-Injected Inertial Electrostatic Confinement Device," Ph.D. Dissertation, Nuclear, Plasma, and Radiological Engineering Dept., University of Illinois at Urbana-Champaign, Champaign, IL, 2013, pp. 30-31.

[14]Ruzic, D. N., *Electric Probes for Low Temperature Plasmas*, The American Vacuum Society Education Committee, American Vacuum Society, New York, 1994, p. 57.

[15]Ko, E. and Hershkowitz, N., "Asymmetry reversal of ion collection by mach probes in flowing unmagnetized plasmas," Plasma Phys. Control. Fusion, Vol. 48, No. 5, 2006, pp. 621-634.

[16]Hutchinson, I. H., *Principles of Plasma Diagnostics*, 2nd ed., Cambridge University Press, New York, 2002, pp. 97-98.

[17]Shabshelowitz, A., "Study of RF Plasma Technology Applied to Air-Breathing Electric Propulsion," Ph.D. Dissertation, Dept. of Aerospace Engineering, University of Michigan, Ann Arbor, MI, 2013, p. 102.

[18]Böhm, C. and Perrin, J., "Retarding-field analyzer for measurements of ion energy distributions and secondary electron emission coefficients in low-pressure radio frequency discharges," Review of Scientific Instruments, Vol. 64, No. 31, 1993, pp. 31-44.